

# Circular RNAs as novel regulators of $\beta$ -cell functions in normal and disease conditions



Lisa Stoll<sup>1</sup>, Jonathan Sobel<sup>1</sup>, Adriana Rodriguez-Trejo<sup>1</sup>, Claudiane Guay<sup>1</sup>, Kailun Lee<sup>2</sup>, Morten Trillingsgaard Venø<sup>3</sup>, Jørgen Kjems<sup>3</sup>, D. Ross Laybutt<sup>2</sup>, Romano Regazzi<sup>1,\*</sup>

## ABSTRACT

**Objective:** There is strong evidence for an involvement of different classes of non-coding RNAs, including microRNAs and long non-coding RNAs, in the regulation of  $\beta$ -cell activities and in diabetes development. Circular RNAs were recently discovered to constitute a substantial fraction of the mammalian transcriptome but the contribution of these non-coding RNAs in physiological and disease processes remains largely unknown. The goal of this study was to identify the circular RNAs expressed in pancreatic islets and to elucidate their possible role in the control of  $\beta$ -cells functions.

**Methods:** We used a microarray approach to identify circular RNAs expressed in human islets and searched their orthologues in RNA sequencing data from mouse islets. We then measured the level of four selected circular RNAs in the islets of different Type 1 and Type 2 diabetes models and analyzed the role of these circular transcripts in the regulation of insulin secretion,  $\beta$ -cell proliferation, and apoptosis.

**Results:** We identified thousands of circular RNAs expressed in human pancreatic islets, 497 of which were conserved in mouse islets. The level of two of these circular transcripts, circHIPK3 and ciRS-7/CDR1as, was found to be reduced in the islets of diabetic *db/db* mice. Mimicking this decrease in the islets of wild type animals resulted in impaired insulin secretion, reduced  $\beta$ -cell proliferation, and survival. ciRS-7/CDR1as has been previously proposed to function by blocking miR-7. Transcriptomic analysis revealed that circHIPK3 acts by sequestering a group of microRNAs, including miR-124-3p and miR-338-3p, and by regulating the expression of key  $\beta$ -cell genes, such as *Slc2a2*, *Akt1*, and *Mtpn*.

**Conclusions:** Our findings point to circular RNAs as novel regulators of  $\beta$ -cell activities and suggest an involvement of this novel class of non-coding RNAs in  $\beta$ -cell dysfunction under diabetic conditions.

© 2018 The Authors. Published by Elsevier GmbH. This is an open access article under the CC BY-NC-ND license (<http://creativecommons.org/licenses/by-nc-nd/4.0/>).

**Keywords** Circular RNA; Diabetes; Insulin; microRNA; Pancreatic islet

## 1. INTRODUCTION

Pancreatic  $\beta$ -cells are the sole source of insulin, a peptide hormone essential to regulation of blood glucose homeostasis. Defective insulin secretion can lead to chronic hyperglycemia and the development of diabetes mellitus [1]. Type 1 Diabetes is characterized by a chronic autoimmune attack of the  $\beta$ -cells resulting in complete (or near complete) insulin deficiency and sustained hyperglycemia [2]. In contrast, Type 2 Diabetes, the most common form of the disease, is caused by the failure of  $\beta$ -cells to cope with systemic insulin resistance elicited by environmental factors [1,3].

$\beta$ -cell dysfunction and failure under diabetic conditions is associated with alterations in the expression of protein-coding and non-coding transcripts. There is already strong evidence indicating that different types of non-coding RNAs, including microRNAs (miRNAs) and long non-coding RNAs, are key players in the regulation of  $\beta$ -cell functions and in the development of diabetes [4,5]. However, the role of the newly discovered class of circular RNAs (circRNAs) remains to be elucidated.

A few circular RNAs have already been identified more than 20 years ago [6], but they were considered the result of rare splicing errors. Contrary to this assumption, recent work revealed the presence of thousands of abundant, endogenous circRNAs in mammalian cells [7]. These transcripts are characterized by a covalently closed loop, which is formed by direct backsplicing in a non-canonical order [6]. CircRNAs are generally not poly-adenylated, lack cap structures, and are expressed in cell-type specific manners [8]. Recent evidence suggests that circRNAs can be translated *in vivo* in a cap-independent manner [9]; however, most circRNAs do not encode for proteins.

Despite their abundance, little is known about the functional role of circRNAs. Some circRNAs, mostly intronic isoforms, control the expression of their parent gene [8,10,11]. In addition, circRNAs can also function via the association to RNA-binding proteins [12], and they might play a role in the regulation of alternative splicing by competing with the splicing of linear transcripts [13]. Some circRNAs have been proposed to act as endogenous miRNA sponges [14]. There are just a few circRNAs containing numerous miRNA seed sites, but new evidence suggests that some circRNAs can act by the combinational

<sup>1</sup>Department of Fundamental Neurosciences, University of Lausanne, Switzerland <sup>2</sup>Diabetes and Metabolism Division, Garvan Institute of Medical Research, Darlinghurst, Sydney, New South Wales, Australia <sup>3</sup>Interdisciplinary Nanoscience Center (iNANO) and Department of Molecular Biology and Genetics, Aarhus University, Denmark

\*Corresponding author. Department of Fundamental Neurosciences, Rue du Bugnon 9, CH-1005 Lausanne, Switzerland. Fax: +41 21 692 52 55. E-mail: [Romano.Regazzi@unil.ch](mailto:Romano.Regazzi@unil.ch) (R. Regazzi).

Received November 20, 2017 • Revision received January 10, 2018 • Accepted January 16, 2018 • Available online 31 January 2018

<https://doi.org/10.1016/j.molmet.2018.01.010>

sponging of several miRNAs [15,16]. In fact, it was demonstrated that circFoxo3 regulates *Foxo3* translation by sponging eight different miRNAs [17] and controls proliferation by producing a ternary complex with p21 and CDK2 [18]. Another example of a miRNA sponge is ciRS-7 (also called CDR1as), which possesses more than 70 binding sites for miR-7 [14], and has been shown to regulate insulin content and secretion of mouse islets [19]. Until now, the latter study represents the only evidence of circRNA control of  $\beta$ -cell activities.

The aim of the present study was to identify circRNAs expressed in pancreatic islets and to elucidate their possible role in the control of  $\beta$ -cells functions. For this purpose, we analyzed the expression of thousands previously annotated circRNAs in human islets and confirmed the expression of four of them in human, mouse, and rat  $\beta$ -cells. We found that circHIPK3 and ciRS-7 are highly abundant in pancreatic islets and display reduced expression in diabetes animal models. Silencing these circular transcripts resulted in impaired  $\beta$ -cell function, pointing to a contribution of altered circHIPK3 and ciRS-7 expression to the development of diabetes mellitus.

## 2. MATERIAL & METHODS

### 2.1. Chemicals

Recombinant mouse IL-1 $\beta$ , BSA, poly-L-lysine, prolactin, Histopaque 1119 and 1077 were purchased from Sigma. Recombinant mouse TNF- $\alpha$  was purchased from Enzo Life Sciences, recombinant mouse IFN- $\gamma$  from R&D Systems, and Hoechst dye 33,342 from Invitrogen.

### 2.2. Animals

10–12 weeks old Wistar Han male rats were obtained from JANVIER LABS, and NOD and NOD/SCID mice at 4 and 8 weeks of age from Charles River Laboratories. 13–16 weeks old C57BL/KsJ *db/db* and C57BL/6J *ob/ob* mice, as well as their respective heterozygous and wildtype control mice were taken from the Garvan Institute breeding colonies [20]. All procedures followed the guidelines issued by the National Health and Medical Research Council of Australia, and of the Swiss research council and veterinary offices.

### 2.3. Human islets

Human islets were provided by the Cell Isolation and Transplantation Centre (University of Geneva) through JDRF award 31-2008-413 and 31-2008-416 (ECIT Islet for Basic Research Program). The use of human islets was approved by the Geneva institutional Ethics Committee.

### 2.4. Tissue expression

For expression analysis, tissues from Wistar Han male rats were blast-frozen in liquid nitrogen and lysed in Qiazol (Qiagen). Afterwards, the samples were homogenized with a tissue ruptor (Qiagen) and RNA isolated using the miRNeasy kit (Qiagen).

### 2.5. Isolation, culture and dissociation of rat islets

Rat islets were isolated by collagenase (Roche) digestion [21] and collected by a Histopaque density gradient. Islets were cultured in RPMI 1640 Glutamax medium (Invitrogen) supplemented with 10% fetal calf serum (Gibco), penicillin 50 U/ml, streptomycin 50  $\mu$ g/ml (Gibco), 1 mM Na Pyruvate (Sigma–Aldrich), and 10 mM Hepes (Sigma). Islets were dispersed using Trypsin-EDTA (Gibco).

### 2.6. Culture of MIN6B1 cells

The murine insulin-secreting cell line MIN6B1 [22] was cultured in DMEM-Glutamax medium (Invitrogen), supplemented with 15% fetal

calf serum (Gibco), 50 U/ml penicillin, 50  $\mu$ g/ml streptomycin (Gibco), and 70  $\mu$ M  $\beta$ -mercaptoethanol (Sigma). The MIN6B1 cells tested negative for mycoplasma contamination.

### 2.7. Microarray and RNA sequencing profiling

For mRNA profiling, RNA from MIN6B1 cells treated for 48 h with circHIPK3 siRNA, and control siRNA was extracted with the miRNeasy kit (Qiagen). Global mRNA expression profiling and data analysis were carried out using Mouse Gene Expression Array v.2 (Arraystar). For circRNA profiling, RNA from human islets was extracted with the RNeasy kit (Qiagen) and treated with RNase R to deplete the samples from the linear transcripts. CircRNA expression profiling and data analysis were carried out using Human CircRNA Array v1.0 (Arraystar). In addition, circular RNAs were annotated in published mouse islet RNA sequencing data (ND samples) [23] as previously described [24]. Conserved circRNA backsplicing was examined by mapping human circRNAs from the human genome (hg19) to the mouse genome (mm10) using UCSC liftOver tool. Afterwards, the mouse islet data set was screened for precise orthologous splicing to obtain the list of conserved circRNAs (GSE105096).

### 2.8. Quantitative real-time PCR and sequencing

For mRNA or circRNA amplification, total RNA isolated using miRNeasy kit (Qiagen) was treated with RQ1 RNase-free DNase (Promega) and reverse transcribed using Moloney murine leukaemia virus (M-MLV) reverse transcriptase, RNase H minus (Promega). Real-time PCR was performed with SsoAdvanced™ Universal SYBR® Green supermix (Biorad) on the CFX Connect Real-Time PCR System (Biorad). The relative expression was normalized to the level of a housekeeping gene. For circRNA amplification divergent primer sets were used. Primer sequences are listed in the supplementary material (Supplementary Table 1). For sequencing, PCR products were cleaned using the Wizard® SV Gel and PCR Clean-Up System (Promega), and sequenced by Microsynth.

For miRNA amplification, total RNA was reverse transcribed using Universal cDNA synthesis kit II (Exiqon) and real-time PCR was performed with ExiLENT SYBR® Green master mix (Exiqon) according to manufacturer's instructions. Primer for miRNA amplification were purchased from Exiqon.

### 2.9. Verification of circularity

MIN6B1 RNA was first subjected to RQ1 RNase-free DNase (Promega) treatment and then incubated for 15 min at 37 °C with 3 U/ $\mu$ g RNase R (Epicentre). Afterwards, RNase R was removed by re-isolating the RNA with the miRNeasy kit (Qiagen).

### 2.10. Cell transfection

Transfection of dissociated rat islet cells or MIN6B1 cells was carried out using Lipofectamine 2000 (Invitrogen) for plasmids or with Lipofectamine RNAiMax (Invitrogen) for oligonucleotides. siRNA sequences are listed in the supplementary material (Supplementary Table 2). *Hipk3* siRNA against exon 16 was purchased from Life Technologies (#S800). All assays were performed 48 h after transfection.

### 2.11. Insulin secretion

Dissociated rat islet cells or MIN6B1 cells were pre-incubated in KREBS buffer containing 25 mM Hepes, 0.1% BSA, and 2 mM glucose for 45 min at 37 °C. Afterwards, the medium was replaced by either KREBS buffer with 2 mM glucose (basal condition) or 20 mM glucose (stimulatory condition). After 45 min, the supernatants were collected. Cellular insulin content was recovered in EtOH acid (75% EtOH, 0.55%

HCl) from cells incubated under basal condition, and protein content in Triton-X lysis buffer from cells under stimulatory condition. The amount of insulin in the samples was assessed by ELISA (Merckodia) and protein content by Bradford Assay (Thermo Fisher).

### 2.12. Immunocytochemistry

Dispersed rat islet cells or MIN6B1 cells were plated on poly-L-lysine-coated coverslips. Proliferation was stimulated with 500 ng/ml prolactin (Sigma—Aldrich) for 48 h. The cells were fixed with methanol and permeabilized with PBS supplemented with 0.05% saponin (Sigma). After 30 min in blocking buffer (PBS, 0.05% saponin, 1% BSA), the cells were incubated for 1 h at room temperature with primary antibodies: 1:1300 rabbit anti-Ki67 (Abcam, #ab15580), 1:100 guinea pig anti-insulin (Dako, #A0564). Subsequently, the cells were incubated for 1 h at room temperature with goat anti-rabbit Alexa Fluor 488 and goat anti-guinea pig Alexa Fluor 555 diluted at 1:500 (Invitrogen: #A11008 and #A21435, respectively). Afterwards, the coverslips were incubated for 10 min with Hoechst 33,342 (Invitrogen) and mounted on glass slides using FluorSave™ Reagent (Millipore). The cells were analyzed with a Zeiss Axio Imager Z1.

### 2.13. Cell death assessment

The fraction of apoptotic cells was determined by counting the cells displaying pycnotic nuclei upon Hoechst staining under a fluorescence microscope (AxioCam MRC5, Zeiss). As a positive control, cell death was induced by cytokine treatment (0.1 ng/ml IL-1 $\beta$ , 10 ng/ml TNF- $\alpha$ , and 30 ng/ml IFN- $\gamma$ ) for 24 h.

### 2.14. Luciferase assay

Luciferase activity was measured in MIN6B1 cells with a dual-luciferase reporter assay (Promega). The RIP-Luciferase reporter plasmid driven by a 600 bp fragment of the rat insulin 2 promoter has been previously described [25]. Renilla luciferase activity from the co-transfected pRL-TK promoter vector (Promega) was used to normalize the firefly activity for transfection efficiency. The renilla luciferase construct containing the 3'UTR of human *MTPN* [26] was kindly provided by Dr. Guido Sebastiani, University of Siena. Renilla luciferase activity was normalized to the firefly activity of the co-transfected pGL3-promoter vector (Promega).

### 2.15. Predictions of miRNA target sites

To detect the presence of putative binding sites for the miRNAs expressed in  $\beta$ -cells (Supplementary Table 3), we scanned the sequence of circHIPK3 with the TargetScan algorithm [27] using default parameters.

### 2.16. Testing circHIPK3 as competing endogenous RNA for miRNA targets

We first retrieved the putative target genes for each miRNA from several sources (DIANA-microT, EIMMo, miRBase, miRanda, miRDB, PicTar, PITA and TargetScan) using the *MultiMir* R package [28]. We then assessed whether the collected putative targets were included in the genes differentially expressed upon circHIPK3 silencing and established if they were up- or downregulated. A significant shift in the distribution of miRNA target expression was assessed using the one-sided Mann Whitney U-test. Then, we computed the total number of targets of each miRNA that are differentially expressed ( $p < 0.05$ ) upon circHIPK3 silencing, the fraction of them that are up- or downregulated, and the ratio of downregulated targets over the number of differentially expressed targets (Supplementary Table 4). We applied the binomial

test, which allows rejecting the  $H_0$  hypothesis that there are as many miRNA targets up- or downregulated upon circHIPK3 silencing. We constructed the  $H_1$  hypotheses as significantly more miRNA targets are downregulated in the circHIPK3 siRNA sample.

### 2.17. miRNA target enrichment analysis

For each miRNA of interest, we estimated the average number of miRNA recognition elements ( $MRE_{obs}$ ) with a perfect seed match (7-mers) present in the 3' UTR (AGILENT WholeGenome 4X44k v2, 3'UTRs downloaded from BioMart [28]) of  $n$  downregulated genes ( $FDR < 0.05$  and fold change  $> 1.2$ ). To obtain an empirical  $p$  value associated with each  $MRE_{obs}$ , we independently estimated 100'000 times the average predicted density of miRNA recognition elements  $MRE_{bg}$  for  $N$  regions of matching length randomly sampled from the 3' UTRs of mouse mRNAs not downregulated in the array (minimum 3'UTR length of 10 bp and a GC content above 20%). The same analysis was also performed using the complete list of miRNAs expressed in  $\beta$ -cells with 1000 iterations (Supplementary Table 5).

### 2.18. Data availability

Circular RNA expression profiling data of human islet cells and the list of circRNAs conserved in mouse islets are available under the GEO accession code GSE105096. Data of whole gene expression profiling of MIN6B1 cells upon circHIPK3 silencing are available under the GEO accession code GSE105097.

### 2.19. Statistical analysis

Data are presented as mean  $\pm$  standard deviation. Normality of data was analyzed using Shapiro—Wilk test. Homogeneity of variances was analyzed using Levene statistics. For statistical comparison to a given value, one-sample Student's  $t$  test was used. For two groups, statistical differences were assessed by two-tailed unpaired Student's  $t$  test. In case of multiple comparisons one-way ANOVA was applied followed by the appropriate parametric or nonparametric post hoc test. Statistical significance was considered for  $p$  values smaller than 0.05 (GraphPad Prism 7, IBM SPSS Statistics 23).

## 3. RESULTS

### 3.1. CircRNAs are abundant in pancreatic islets and insulin-secreting cell lines

To investigate the potential involvement of circRNAs in the regulation of  $\beta$ -cell functions, we searched for circular transcripts expressed in human islet samples using a microarray approach. The array includes probes spanning over the circularized junction of 5396 previously annotated circRNAs [6,29]. We detected 3441 of these transcripts in human islet samples (GSE105096).

The analysis of our previously published RNA sequencing data [23], revealed that 497 of them possess precise orthologues expressed in mouse islets (GSE105096). From this list, we picked three circRNAs for further analysis. We chose the most abundant circRNA, circHIPK3, which originates from an exonic sequence of *Hipk3*, and randomly selected two circRNAs from the top 100 expressed circRNAs, which derive from sequences of *Arhgap12* and *Aff1*. We also included in our study ciRS-7/CDR1as, a circRNA which is proposed to act as a sponge for miR-7 and is involved in the regulation of insulin secretion and  $\beta$ -cell proliferation [30,31] (Supplementary Table 6).

The expression of each of these circRNAs in  $\beta$ -cell lines and primary islet cells was confirmed using divergent primers. We indeed detected ciRS-7 (in agreement with a previous report [32]), along with

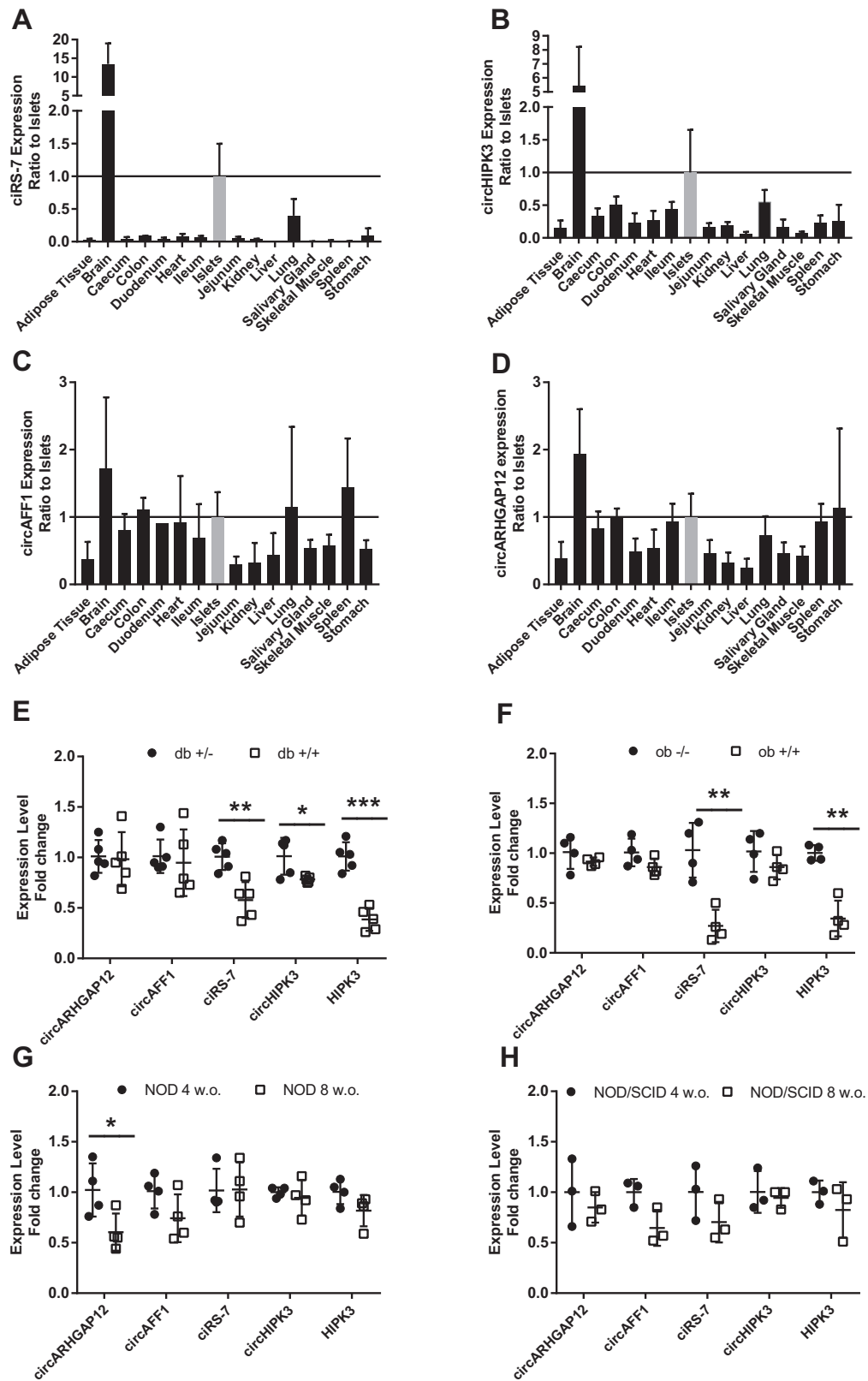


**Figure 1: circRS-7, circAFF1, circARHGAP12 and circHIPK3 expression across rat tissues and in animal models for diabetes.** The expression level of (A) circRS-7, (B) circHIPK3, (C) circAFF1, and (D) circARHGAP12 in 16 different rat tissues was assessed by qPCR. The expression was normalized to islet levels (n = 4). (E–H) RNA expression measured by qPCR in (E) 13–16 weeks old *db/db* mice (*db*<sup>+/+</sup>) versus heterozygous control mice (*db*<sup>+/-</sup>) (n = 5), (F) 13–16 weeks old *ob/ob* mice (*ob*<sup>+/+</sup>) compared to wildtype control (*ob*<sup>-/-</sup>) (n = 4), (G) 4 and 8 weeks old NOD mice (n = 4), and (H) 4 and 8 weeks old NOD/SCID mice (n = 3). The expression levels were compared using unpaired Student's *t*-test. Data are represented as mean ± s.d. \**p* < 0.05, \*\**p* < 0.01, \*\*\**p* < 0.001.

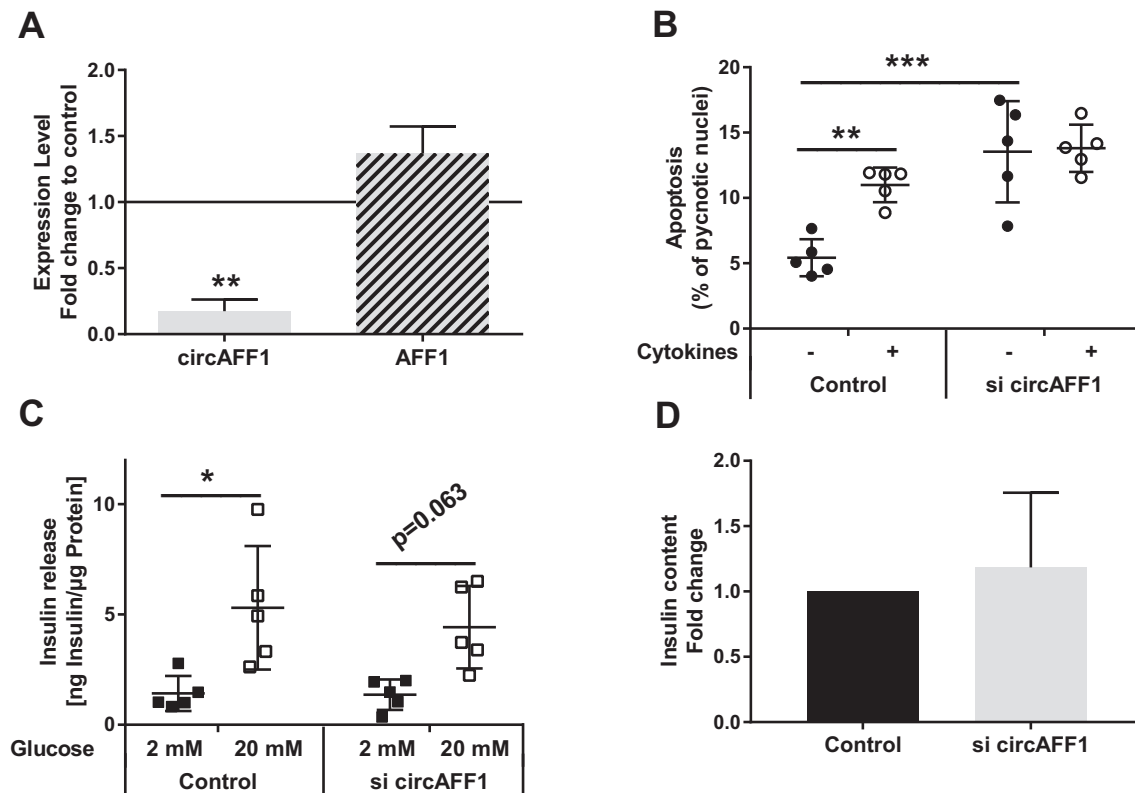


**Figure 2: circAFF1 controls apoptosis of  $\beta$ -cells.** (A–D) Dissociated rat islet cells were transfected with circAFF1 siRNA for 48 h. (A) RNA levels measured by qPCR. Statistical significance was assessed by one-sample Student's *t*-test ( $n = 3$ ). (B) Apoptosis levels with or without cytokine addition for 24 h. Apoptosis was assessed by counting the cells displaying pycnotic nuclei ( $n = 5$ ). Statistical significance was evaluated by one-way ANOVA followed by Games–Howell post hoc. (C–D) Insulin secretion (C) and insulin content (D) were assessed upon treatment with either 2 mM or 20 mM glucose ( $n = 5$ ). Statistical significance in insulin secretion was evaluated by one-way ANOVA followed by Games–Howell post hoc. Statistical significance in insulin content was calculated by one-sample Student's *t*-test. Data are represented as mean  $\pm$  s.d. \* $p < 0.05$ , \*\* $p < 0.01$ , \*\*\* $p < 0.001$ .

circARHGAP12, circAFF1, and circHIPK3 in the insulin-secreting cell lines INS832/13, and MIN6B1, as well as, in mouse, rat, and human islets. Sequencing of the PCR products confirmed the expected amplification of the circularized junction of the circRNAs (data not shown). To further verify that these transcripts are truly circular, we treated MIN6B1 samples with RNase R, an exonuclease that efficiently degrades linear but not circular RNAs [33]. As expected, circHIPK3, circAFF1, and circARHGAP12 were more resistant to RNase R than their linear counterparts. Moreover, ciRS-7 was more resistant to the treatment than *Gapdh* (there is no corresponding linear transcript of ciRS-7 expressed in  $\beta$ -cells) (Supplementary Figure 1). Taken together, these observations confirm the expression of these circular transcripts in insulin-secreting cells.

### 3.2. Differential expression of circRNAs in rat tissues

Some circRNAs have been shown to follow a specific tissue distribution pattern [8]. For this reason, we measured the level of the selected circRNAs in different rat tissues (Figure 1A–D). In line with previous reports [29], ciRS-7 was found to be expressed at the highest level in brain, at medium level in islets, and at lower levels in the remaining tissues (Figure 1A). CircHIPK3 was detected in most tissues but was most abundant in brain and pancreatic islets (Figure 1B). Finally, circAFF1 and circARHGAP12 were expressed at similar levels across all the examined tissues (Figure 1C,D).

### 3.3. Expression of the circRNAs in mouse models of Type 1 and Type 2 diabetes

We measured the expression of the selected circRNAs in the islets of different diabetes animal models. We found that circHIPK3 displays decreased expression in diabetic *db/db* mice (Figure 1E), while the level of ciRS-7 is reduced both in *db/db* and in *ob/ob* mice, which are obese but still normoglycemic (Figure 1E,F). Consistent with data obtained in the islets of Type 2 diabetic donors [34], the expression of linear *Hipk3* was also diminished in both models. The level of circARHGAP12 and circAFF1 was not altered in Type 2 Diabetes models, but a reduction in the expression of circARHGAP12 was observed in the islets of prediabetic NOD mice, which spontaneously develop Type 1 Diabetes (Figure 1G). The expression of circARHGAP12 was unchanged in age-matched NOD/SCID mice which do not develop the disease (Figure 1H), indicating that the observed reduction is not an age-related effect.

### 3.4. Role of the selected circRNAs in the control of $\beta$ -cell activities

We then assessed whether these circRNAs are required to accomplish specialized  $\beta$ -cells functions. For this purpose, we silenced each of these transcripts using siRNAs directed against the circularized junctions or against sequences specific to the circRNAs, and tested the impact on insulin biosynthesis and secretion,  $\beta$ -cell survival, and proliferation, which are dysregulated under diabetic conditions.

We found that a siRNA specifically silencing circARHGAP12 and without any effect on the expression of the corresponding linear transcript generated from the *Arhgap12* locus (Supplementary Figure 2a) has no effect on proliferation, survival, or insulin secretion of MIN6B1 cells (Supplementary Figure 2b–e). Therefore, the functional role of this transcript was not further investigated.

Silencing of circAFF1 in MIN6B1 cells or primary rat  $\beta$ -cells (Supplementary Figure 3a, Figure 2A) resulted in an increase in apoptosis comparable to that observed after treatment of the cells with a combination of proinflammatory cytokines (Supplementary Figure 3b, Figure 2B). In contrast, circAFF1 silencing did not affect the proliferative capacity of MIN6B1 cells (Supplementary Figure 3c), and did not

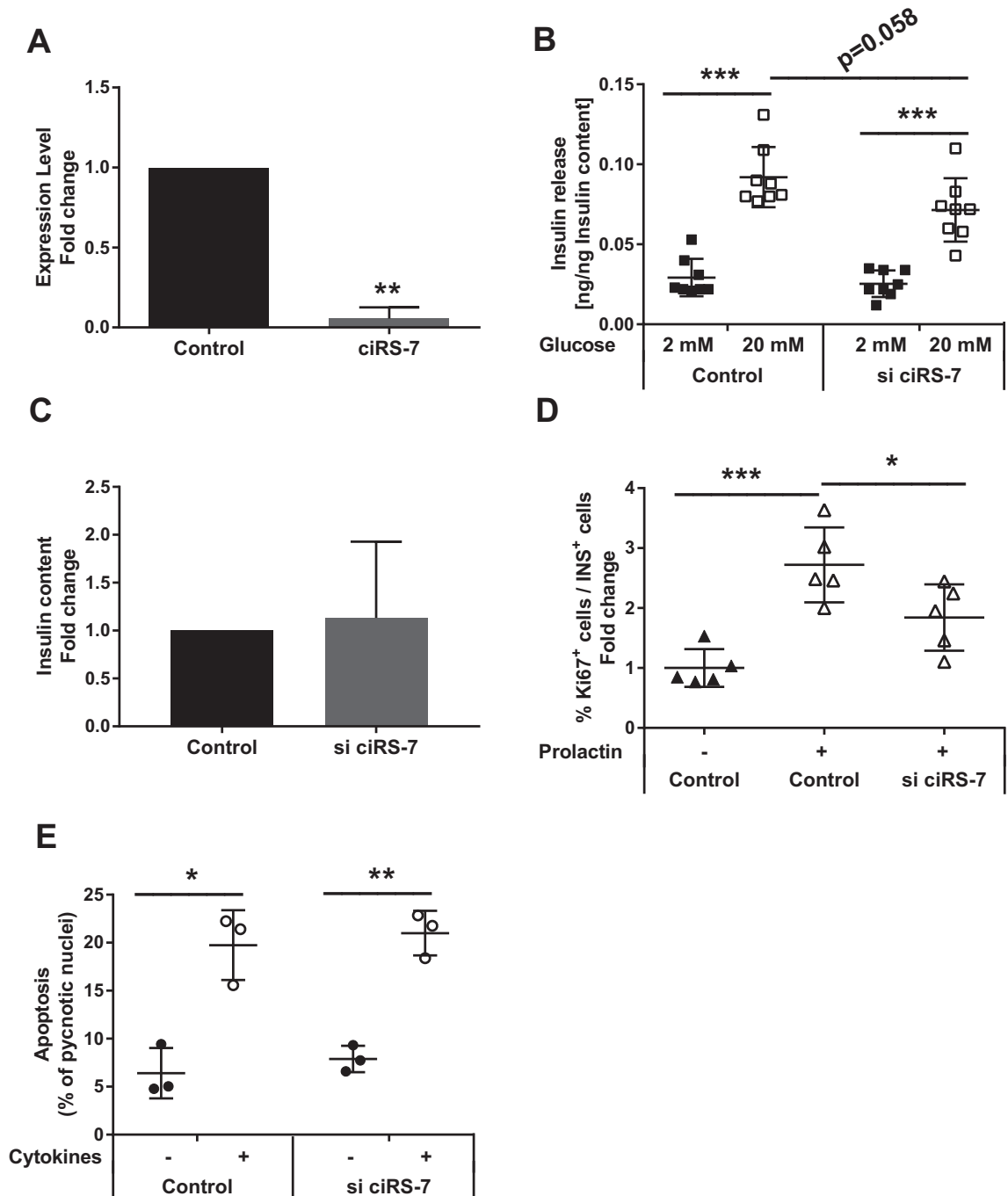


**Figure 3: Role of ciRS-7 in the control of  $\beta$ -cell functions.** Dissociated rat islet cells (A–D) were treated with ciRS-7 siRNA for 48 h. (A) ciRS-7 levels measured by qPCR. Statistical significance was assessed by one-sample Student's *t*-test ( $n = 3$ ). (B–C) Insulin secretion (B) and insulin content (C) were assessed upon treatment with either 2 mM or 20 mM glucose ( $n = 8$ ). Statistical significance in insulin secretion was evaluated by one-way ANOVA followed by Tukey post hoc. Statistical significance in insulin content was assessed by one-sample Student's *t*-test. (D) Proliferation with or without prolactin stimulation was measured by Ki67-staining of insulin-positive cells ( $n = 5$ ). Statistical significance was assessed by one-way ANOVA followed by Dunnett-T test. (E) Apoptosis levels with or without cytokine addition for 24 h. Apoptosis was assessed by counting the cells displaying pycnotic nuclei ( $n = 3$ ). Statistical significance was evaluated by one-way ANOVA followed by Games–Howell post hoc. Data are represented as mean  $\pm$  s.d. \* $p < 0.05$ , \*\* $p < 0.01$ , \*\*\* $p < 0.001$ .

alter insulin content or secretion in response to glucose of MIN6B1 cells or of primary rat  $\beta$ -cells (Supplementary Figure 3d–e, Figure 2C–D).

Xu et al. observed that overexpression of ciRS-7 in MIN6 and mouse islet cells results in an increase in insulin secretion and content, while overexpression of miR-7 had the opposite effect [32]. As we found a reduction in ciRS-7 level in the islets of *db/db* and *ob/ob* mice, we reproduced the decreased expression in wild type  $\beta$ -cells (Figure 3A) and observed that insulin secretion tends to be reduced ( $p = 0.058$ ) while insulin content is unaffected (Figure 3B,C).

Since miR-7 has been shown to control proliferation, we also investigated whether the modulation of ciRS-7 levels affects  $\beta$ -cell replication.

Indeed, silencing of ciRS-7 diminished prolactin-stimulated proliferation of primary rat  $\beta$ -cells (Figure 3D) without affecting the survival rate (Figure 3E). We performed the same assays in MIN6B1 cells using a different siRNA resulting in a similar functional impact (Supplementary Figure 4a–e). These data suggest that alterations of ciRS-7 levels under diabetic conditions may contribute to  $\beta$ -cell dysfunction.

circHIPK3 is one of the most abundant circRNAs expressed in pancreatic islets. Using a siRNA directed against the circular junction, we efficiently silenced circHIPK3 in both MIN6B1 cells and rat islets (Figure 4A, Figure 5B), resulting in an increase in apoptosis (Supplementary Figure 5a, Figure 4B) and in a negative impact on the proliferative capacity of the cells. Indeed, prolactin failed to stimulate

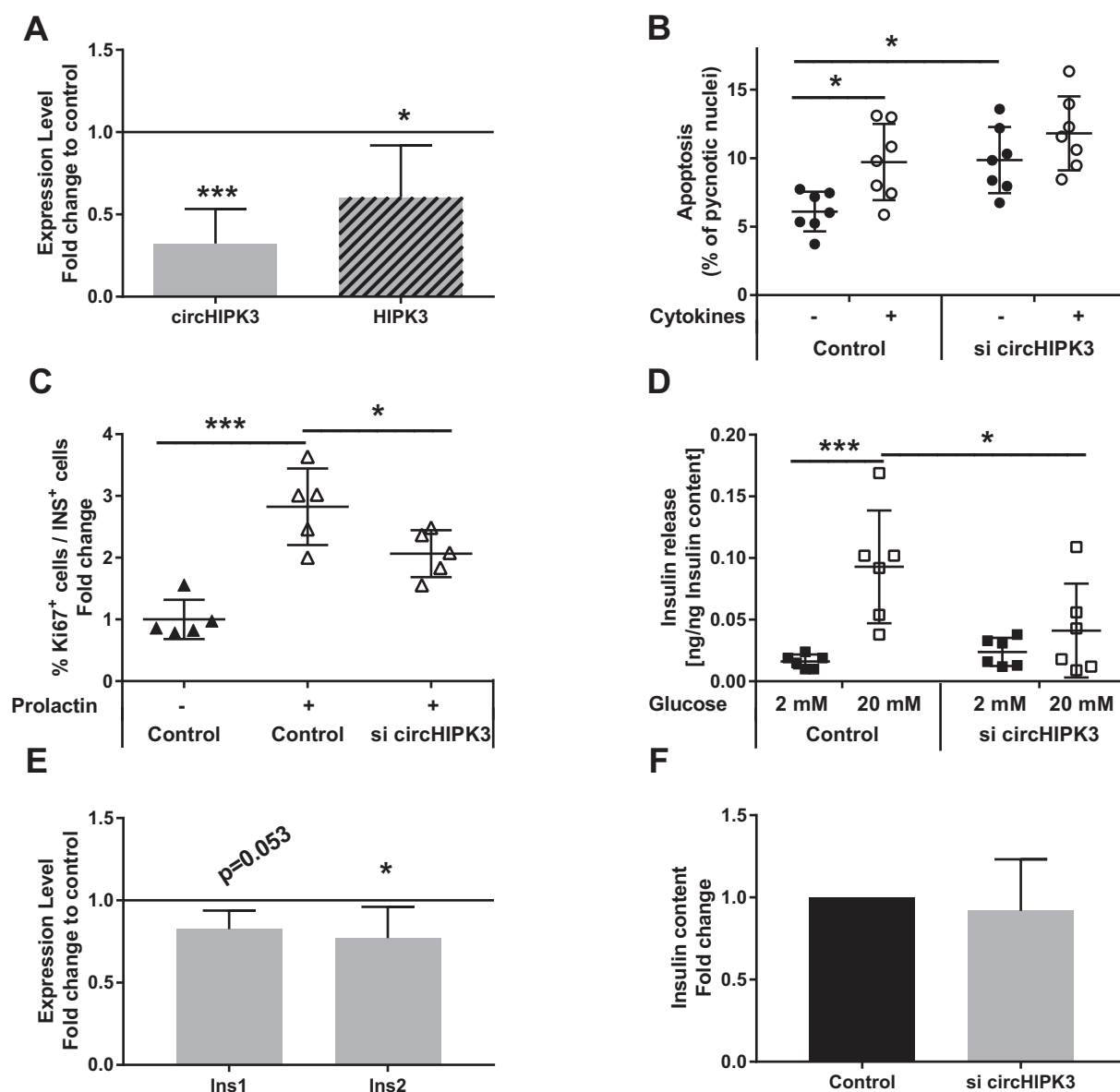


**Figure 4: Circular HIPK3 regulates apoptosis, proliferation, and insulin secretion of  $\beta$ -cells.** (A–F) Dissociated rat islet cells were treated with circHIPK3 siRNA for 48 h. (A) circHIPK3 and *Hipk3* levels measured by qPCR ( $n = 7$ ). (B) Apoptosis levels with or without cytokine addition for 24 h. Apoptosis was assessed by counting the cells displaying pycnotic nuclei ( $n = 7$ ). Statistical significance was evaluated by one-way ANOVA followed by Tukey post hoc. (C) Proliferation was measured by Ki67-staining of insulin-positive cells with or without prolactin stimulation ( $n = 5$ ). Statistical significance was assessed by one-way ANOVA followed by Dunnett-T test. (D;F) Insulin secretion (D) and insulin content (F) were assessed upon treatment with either 2 mM or 20 mM glucose ( $n = 6$ ). Statistical significance in insulin secretion was evaluated by one-way ANOVA followed by Tukey post hoc. Statistical significance in insulin content was assessed by one-sample Student's *t*-test. (E) *Ins1* and *Ins2* levels were measured by qPCR. Statistical significance was assessed by one-sample Student's *t*-test. Data are represented as mean  $\pm$  s.d. \* $p < 0.05$ , \*\* $p < 0.01$ , \*\*\* $p < 0.001$ .

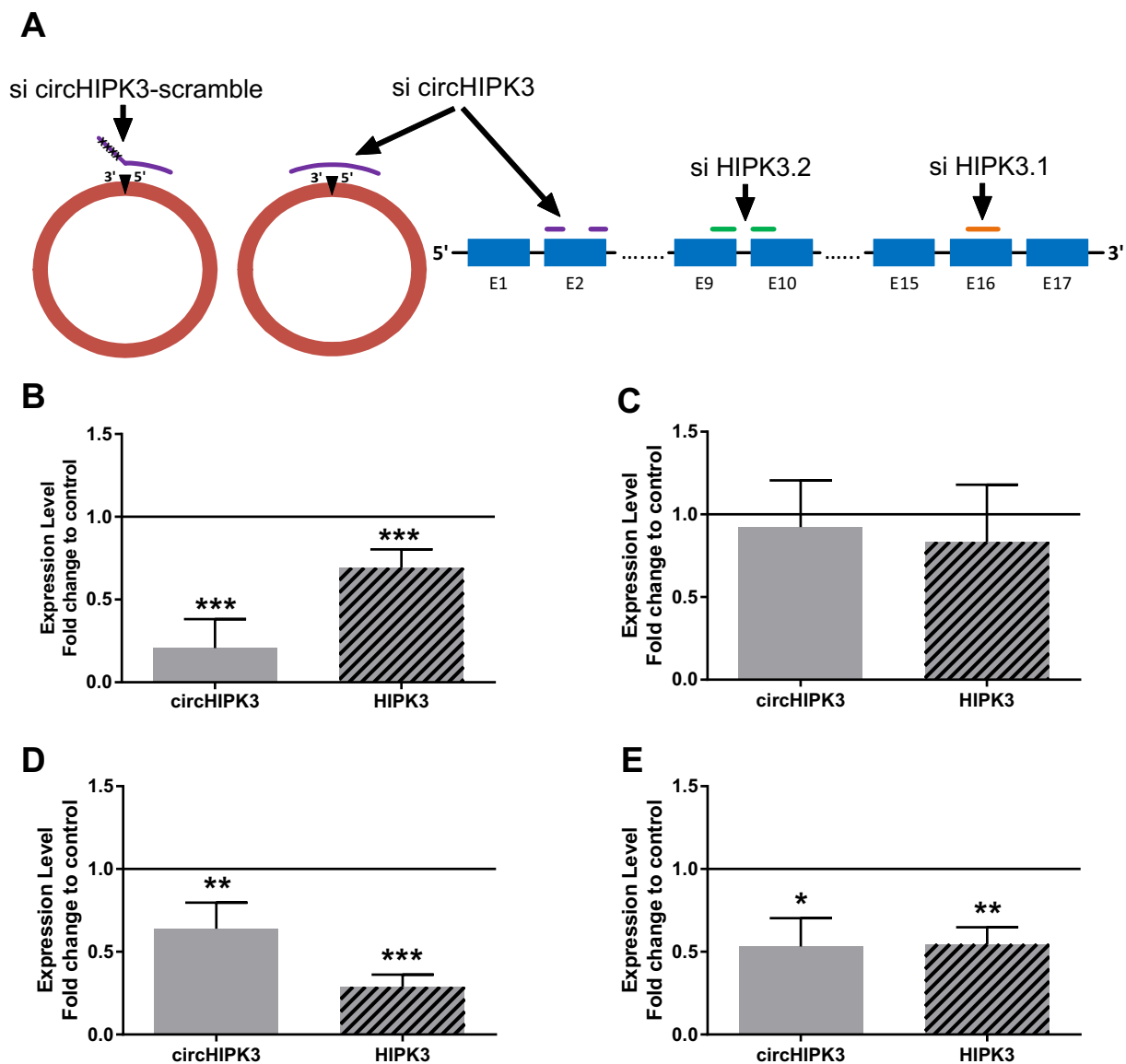


**Figure 5: The expression of circular and linear HIPK3 is interconnected.** (A) Schematic representation of circHIPK3 and *Hipk3* siRNAs binding sites on circHIPK3 and *Hipk3* sequence. (B–E) circHIPK3 and *Hipk3* levels measured by qPCR in MIN6B1 cells 48 h after transfection with circHIPK3 siRNA (n = 7) (B), circHIPK3 scrambled siRNA (n = 6) (C), *Hipk3* siRNA directed against exon 16 (si HIPK3.1) (n = 6) (D), and *Hipk3* siRNA directed against the splice junction of exons 9 and 10 (si HIPK3.2) (n = 3) (E). Statistical significance was assessed using one-sample Student's *t*-test. Data are represented as mean  $\pm$  s.d. \**p* < 0.05, \*\**p* < 0.01, \*\*\**p* < 0.001.

proliferation of MIN6B1 and primary  $\beta$ -cells containing lower levels of this circRNA (Supplementary Figure 5b, Figure 4C). Furthermore, upon silencing of circHIPK3, insulin secretion in response to glucose was impaired (Figure 4D, Supplementary Figure 5c) and *Insulin* mRNA levels were significantly lower (Figure 4E, Supplementary Figure 5d). This resulted in a decrease in insulin content in MIN6B1 cells, but not in rat islets (Supplementary Figure 5e, Figure 4F). These observations indicate that appropriate circHIPK3 levels are necessary to maintain optimal  $\beta$ -cell functions.

### 3.5. Interconnection of circular and linear *Hipk3* isoforms

Since circHIPK3 is involved in the control of important  $\beta$ -cell functions, the mechanism through which this circular transcript exerts its regulatory activity was investigated in more detail.

Surprisingly, we found that, albeit to a lesser extent, linear *Hipk3* mRNA levels are significantly decreased upon silencing of circHIPK3 in

rat islets and MIN6B1 cells (Figure 4A, Figure 5B). In the linear *Hipk3* transcript, the sequence targeted by the siRNA against circHIPK3 matches two short separate segments located at the 5' and 3' ends of exon 2 and should thus not be targeted by the RISC complex (Figure 5A). Nonetheless, to ensure that these partially matching sequences are not sufficient to silence linear *Hipk3*, we designed a siRNA targeting the 14 nucleotides at the 5' end of linear *Hipk3* with the remaining nucleotides being scrambled (si circHIPK3-scramble) (Figure 5A). This siRNA did neither affect the expression of circHIPK3 nor of linear *Hipk3* (Figure 5C). These results confirm that circHIPK3 siRNA can directly silence only the circular transcript and indicate that changes in the expression of linear *Hipk3* are indirectly caused by the drop in circHIPK3 levels. Remarkably, we found that the opposite was also true. Indeed, a siRNA targeting an exonic sequence of linear *Hipk3* (exon 16, si HIPK3.1) (Figure 5A), that is not included in circHIPK3 sequence, not only lowered *Hipk3* mRNA but also the level of circHIPK3

(Figure 5D). To exclude that this siRNA reduces circHIPK3 by affecting the pre-spliced RNA, we designed a different *Hipk3* siRNA directed against the splice junction between exons 9 and 10, which cannot bind to the un-spliced RNA (si HIPK3.2) (Figure 5A). Likewise, this siRNA decreased the levels of both linear *Hipk3* and circHIPK3 (Figure 5E) confirming that the expression of the two transcripts is tightly linked. Due to the interconnection of circHIPK3 and *Hipk3* expression we wondered whether the functional effect observed upon silencing of circHIPK3 is indirectly mediated by the decrease in *Hipk3* levels. Interestingly, linear *Hipk3* displays an expression pattern similar to

circHIPK3, being higher in islets than in all the other analyzed tissues (Supplementary Figure 6a). Shojima et al. investigated the role of HIPK3 in the control of insulin secretion in *Hipk3*<sup>-/-</sup> mice [35]. They observed that both insulin content and glucose-stimulated insulin secretion are decreased in *Hipk3* knockout mice and in wild-type mouse islets treated with a siRNA against *Hipk3*. In our hands, silencing of *Hipk3* in MIN6B1 cells did not alter insulin secretion, yet insulin content was significantly decreased (Figure 6A,B). Similar to circHIPK3, silencing of linear *Hipk3* reduced *Insulin* mRNA levels (Figure 6C), as well as, insulin promoter activity in MIN6B1 cells

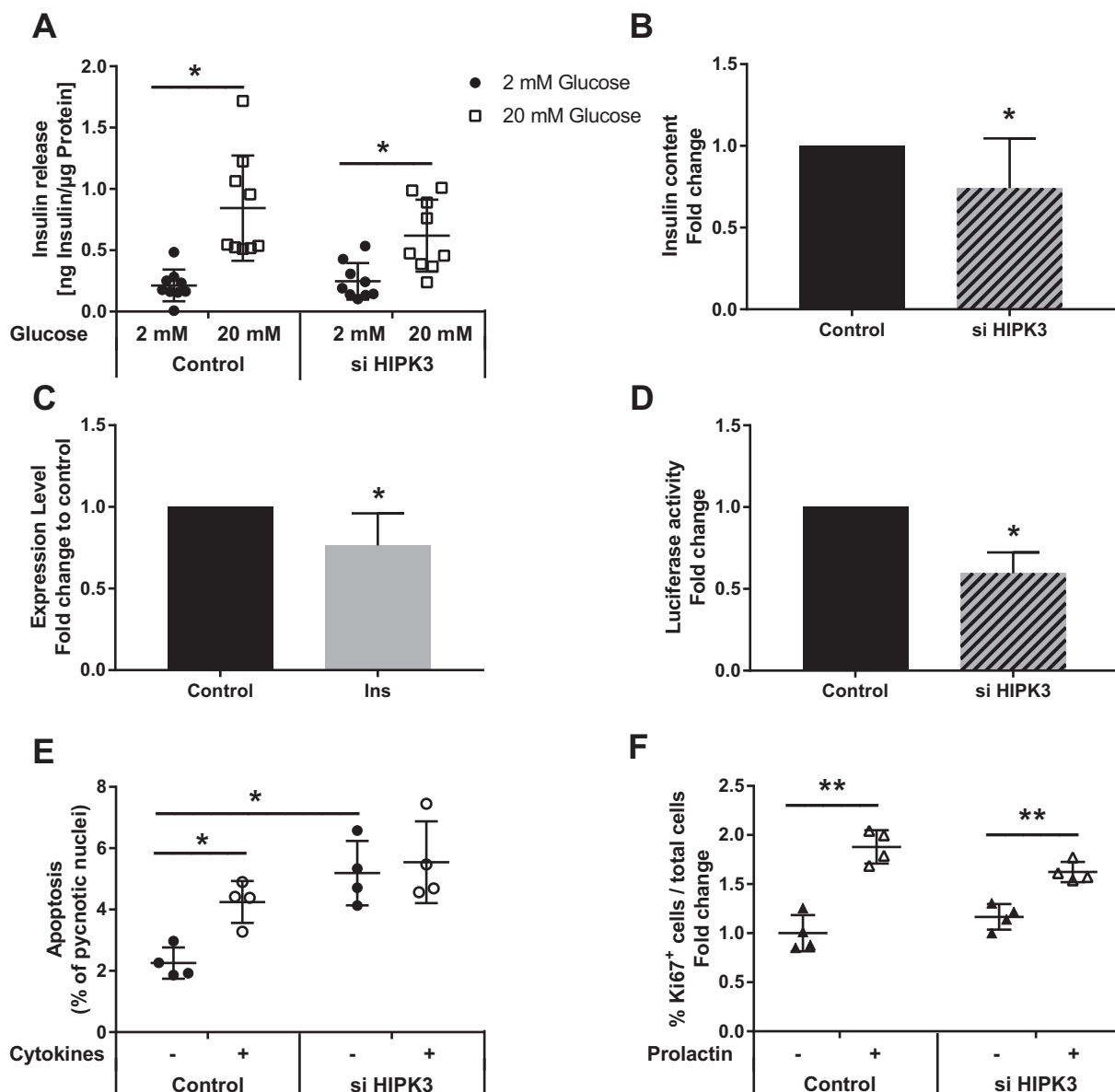


**Figure 6: HIPK3 controls apoptosis and insulin secretion of  $\beta$ -cells.** (A–F) MIN6B1 cells were treated for 48 h with *Hipk3* siRNA. (A–B) Insulin secretion (A) and insulin content (B) were assessed upon treatment with either 2 mM or 20 mM glucose ( $n = 9$ ). Statistical significance in insulin secretion was evaluated by one-way ANOVA followed by Games–Howell post hoc. Statistical significance in insulin content was calculated by one-sample Student’s *t*-test. (C) *Ins* level measured by qPCR ( $n = 6$ ). Statistical significance was assessed using one-sample Student’s *t*-test. (D) Rat insulin promoter activity was measured 48 h after transfection with a firefly luciferase construct driven under the control of the rat insulin promoter ( $n = 3$ ). Statistical significance was assessed using one-sample Student’s *t*-test. (E) Apoptosis was evaluated by counting the cells displaying pycnotic nuclei with or without cytokine addition for 24 h ( $n = 4$ ). Statistical significance was assessed by one-way ANOVA followed by Games–Howell post hoc. (F) Proliferation was measured by Ki67-staining with or without prolactin stimulation ( $n = 4$ ). Statistical significance was assessed by one-way ANOVA followed by Games–Howell post hoc. Data are represented as mean  $\pm$  s.d. \* $p < 0.05$ , \*\* $p < 0.01$ , \*\*\* $p < 0.001$ .

(Figure 6D) without affecting the expression of several transcription factors known to control insulin biosynthesis (Supplementary Figure 6b). Furthermore, silencing of linear *Hipk3* in MIN6B1 cells induced apoptosis similar to circHIPK3 (Figure 6E). However, the proliferative capacity was not reduced in MIN6B1 cells after silencing of *Hipk3* and stimulation with prolactin (Figure 6F). These data indicate that circHIPK3 and *Hipk3* have similar impacts on  $\beta$ -cell activities.

### 3.6. CircHIPK3 regulates the expression of key $\beta$ -cell genes

We then carried out a series of experiments to determine the mode of action of circHIPK3. We first assessed whether this circular transcript controls *Insulin* mRNA levels by affecting the activity of the insulin promoter. Indeed, we found that the activity of the insulin promoter is altered by modulating the level of circHIPK3 in MIN6B1 cells (Figure 7A). Nevertheless, the expression of several transcription factors controlling *Insulin* mRNA was not modified by circHIPK3 knockdown, indicating that circHIPK3 is likely to act at the translational or post-translational level (Figure 7B).

To obtain a broader picture of the mechanisms underlying the multiple effects of circHIPK3, we analyzed by microarray the global mRNA expression changes caused by the silencing of this circular transcript (GSE105097). Consistent with the observed functional effects, pathway analysis of the differentially expressed transcripts revealed a downregulation of genes involved in insulin secretion (Supplementary Figure 6c). Surprisingly, the main upregulated pathway was olfactory signaling, which was previously shown to be associated to Type 2 Diabetes and paternal high fat diet [36,37]. The changes in the expression of several key genes, including *Akt1*, *Slc2a2*, and *Mtpn*, which are downregulated upon circHIPK3 silencing, were confirmed by qPCR (Supplementary Figure 6d). Similar changes in gene expression upon circHIPK3 knockdown were also detected in rat (Figure 7C) and in human islets (Figure 7D). Taken together, these data show that circHIPK3 regulates glucose-stimulated insulin secretion, insulin biosynthesis, proliferation, and apoptosis by affecting the expression of key genes associated with these functions. Interestingly, except for *Cckar*, silencing of the linear *Hipk3* transcript did not affect the expression of these genes (Figure 7E), indicating that linear HIPK3 and circHIPK3 might act via different pathways.

### 3.7. Part of the effects of circHIPK3 may be mediated via miRNA sponging

CircHIPK3 has been proposed to act as a sponge for several miRNAs [15,38], many of which control the activities of  $\beta$ -cells. To assess to what extent the changes in mRNA expression observed upon circHIPK3 silencing may be driven by miRNA sponging, we used a computational approach to identify miRNA seed sites present within the sequence of this circRNA. We found that circHIPK3 contains potential binding sites for several miRNAs expressed in  $\beta$ -cells (Supplementary Figure 7a, Supplementary Table 3). We then exploited our microarray data by analyzing the level of all the genes targeted by these miRNAs displaying changes  $>1.2$  fold and a  $p$ -value  $< 0.05$  after circHIPK3 silencing. In line with the sponge hypothesis, the putative targets of several miRNAs expressed in  $\beta$ -cells were preferentially downregulated upon silencing of circHIPK3 using a binomial test (Supplementary Figure 7b and c, Supplementary Table 4). The distribution of the targets of 59 of these miRNAs was also significantly reduced using a one sided Mann–Whitney U-test (Figure 8A,B, Supplementary Table 4). At the top of this list we found miRNAs with known functions in  $\beta$ -cells, which have been previously shown to bind to circHIPK3, namely miR-124-3p, miR-338-3p, miR-29b-3p, and miR-30 [15,39–44].

For these miRNAs, the number of targets within the differentially expressed genes ranges from 28 for miR-338-3p to 242 for miR-124-3p, out of which most are downregulated (Figure 8A–C). To verify the relevance of this effect, we ran the same analysis for two other abundant miRNAs, miR-7-5p and miR-375-3p, which possess several putative targets within the differentially expressed genes. In this case, we did not find any significant enrichment toward downregulation (Figure 8A–C). To further confirm these observations, we performed a miRNA-target enrichment analysis using a random sampling procedure. For this purpose, we compared the number of miRNA response elements (MRE) in the 3'UTRs of the significantly downregulated genes (FDR  $< 0.05$ ) (MREobs) with the number of miRNA response elements in 3'UTRs of genes unaffected upon circHIPK3 silencing (MREbg) (Supplementary Table 5). Using this computational approach, that takes into account potential bias due to differences in the 3'UTR length and GC content, we confirmed an enrichment of miR-338-3p and miR-124-3p binding sites in the 3'UTRs of the downregulated genes (Figure 8D).

To elucidate whether circHIPK3 can indeed sponge these miRNAs, we first measured the expression of these miRNAs upon silencing of circHIPK3. We found that a decrease in circHIPK3 level does not affect the levels of miR-124-3p, miR-338-3p or miR-29b (Figure 7F). Since miRNA sponging does not imply changes in the expression of the respective miRNA [45], we analyzed the activity of a luciferase construct containing the 3'UTR of human *MTPN*, which has been shown to be controlled by miR-124-3p [39]. Indeed, silencing of circHIPK3 resulted in a drop in luciferase activity consistent with a rise in the repressive activity of miR-124-3p (Figure 7G).

Taken together, these data indicate that the gene expression changes observed upon circHIPK3 silencing could at least partly be mediated by increasing the repressive activity of a group of miRNAs that control the functions of  $\beta$ -cells, including miR-124-3p and miR-338-3p.

## 4. DISCUSSION

In this study, we detected more than 3000 previously annotated circRNAs, showing that these transcripts are abundant in islets. Recent estimates indicate that human cells may express up to 160,000 circRNAs [15,46]. Therefore, the array is likely to cover only a small fraction of the circRNAs expressed in human islet cells. We were able to detect about 500 (14.4%) of these circRNAs in RNA sequencing data from mouse islets, indicating that at least a fraction of them is evolutionary conserved. A similar degree of conservation has been observed by Memczak et al. comparing circRNAs expressed in human and mouse cells [29].

We selected four exonic circRNAs for further investigations and, in line with previous reports [47], we found that their sequences were well conserved between rat, mouse, and human cells. The analysis of the level of these circRNAs in different Type 1 and Type 2 Diabetes models revealed that circARHGAP12 expression is reduced in the islets of prediabetic NOD mice. The functional role of this circRNA in  $\beta$ -cells remains to be defined since silencing of this transcript does not affect proliferation, apoptosis, or insulin secretion. The level of circAFF1 is unaffected in the investigated diabetes models but silencing of circAFF1 led to apoptosis. Future experiments will need to determine whether the expression of this transcript is modulated in pathological conditions associated with alterations in  $\beta$ -cell survival.

ciRS-7 and circHIPK3, two of the studied circRNAs that are highly abundant in pancreatic islets, were found to be differentially expressed under diabetic conditions and to play important roles in the control of  $\beta$ -cell functions. The level of ciRS-7 is decreased both in *ob/ob* and *db/db* mice, which are severely obese due to the lack of leptin or of the

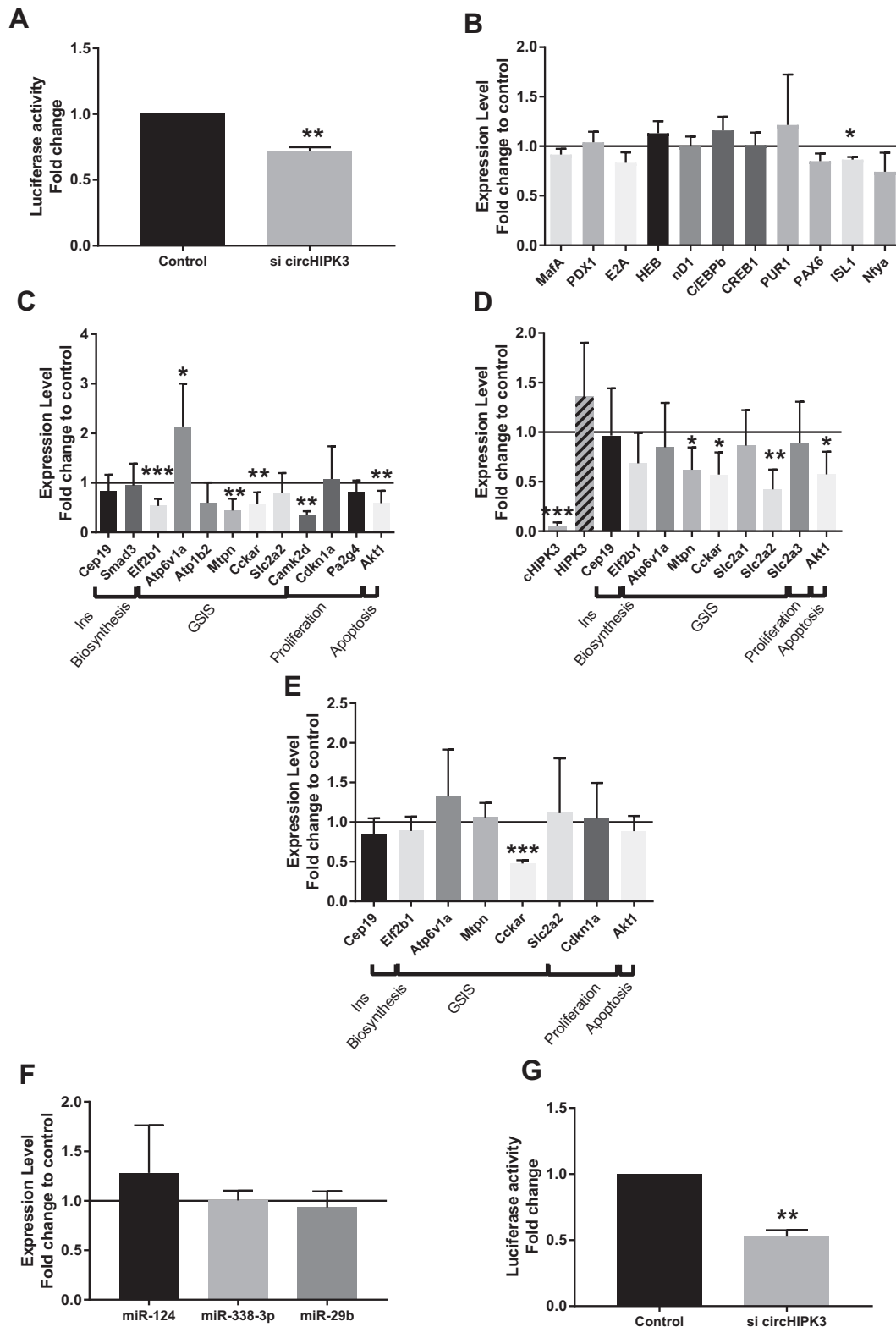


**Figure 7: CircHIPK3 regulates the expression of important genes controlling  $\beta$ -cell functions.** (A) Rat insulin promoter activity was measured 48 h after transfection with a firefly luciferase construct driven under the control of the rat insulin promoter and circHIPK3 siRNA ( $n = 3$ ). Statistical significance was assessed using one-sample Student's  $t$ -test. MIN6B1 cells (B,E–G), dispersed rat islet cells (C) or dispersed human islet cells (D) were transfected for 48 h with circHIPK3 siRNA (B–D, F–G) or *Hipk3* siRNA (E). (B–F) RNA level measured by qPCR ( $n = 3–7$ ). Statistical significance was assessed using one-sample Student's  $t$ -test. (G) Activity of a luciferase construct containing the 3' UTR of human *MTPN* ( $n = 3$ ). Statistical significance was assessed using one-sample Student's  $t$ -test. Data are represented as mean  $\pm$  s.d. \* $p < 0.05$ , \*\* $p < 0.01$ , \*\*\* $p < 0.001$ .

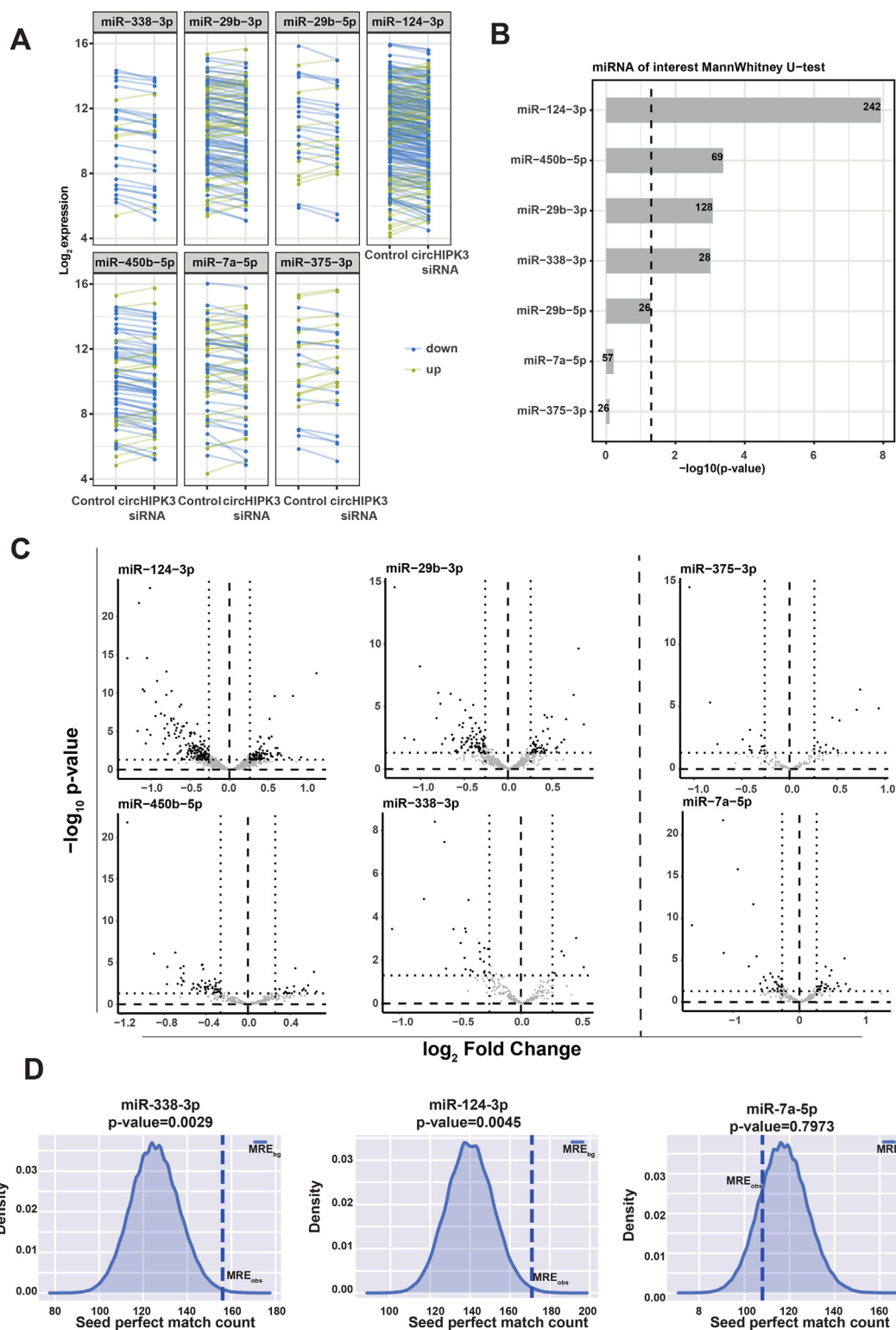


**Figure 8: circHIPK3 might sponge miRNAs in MIN6B1 cells.** (A) Expression of predicted miRNA targets significantly changing in circHIPK3 siRNA samples versus control samples measured by microarray. (B) Statistical analysis of the distribution of predicted miRNA targets significantly changing in circHIPK3 siRNA versus control samples. Bars represent  $-\log_{10}$  p-value of the one-sided Mann Whitney U-test for several miRNAs. Number of predicted miRNA targets are indicated within each bar. (C) Differential expression analysis of control versus circHIPK3 siRNA samples of predicted miRNA targets represented with the  $\log_2$  fold-change and  $-\log_{10}$  p-value. Significantly changing miRNA targets are displayed with black dots, not significantly changing targets with grey dots. The dotted lines represent the thresholds used for the analysis ( $p$ -value < 0.05 and absolute fold change > 1.2). (D) MiRNA target enrichment analysis for miR-338-3p and miR-124-3p, as well as, miR-7a-5p as a control. Number of miRNA response elements in the 3'UTRs of significantly downregulated genes (MRE<sub>obs</sub>) was compared to 3'UTRs of not significantly changing genes (MRE<sub>bg</sub>). Significance was computed by comparing MRE<sub>obs</sub> versus MRE<sub>bg</sub> using random sampling analysis.

leptin receptor, respectively. In contrast to *db/db* mice, which are diabetic, *ob/ob* mice are able to compensate for the increased insulin demand linked to obesity but are nonetheless prone to diabetes development. Therefore, the decrease in ciRS-7 levels observed in *ob/ob* and *db/db* mice is consistent with an involvement in diabetes development. CiRS-7 has been proposed to act as a sponge for miR-7 [48]. In agreement with this hypothesis, Piwecka et al. observed a deregulation of miR-7 in ciRS-7 knock-out mice probably due to the lack of stabilisation of this miRNA by the circular transcript [49]. CiRS-7 also possesses 22 seed sites for the miR-876-5p/3167 family [14], but these miRNAs are not expressed in  $\beta$ -cells and are unlikely to contribute to the functional effects of ciRS-7. Overexpression of ciRS-7 has been reported to increase glucose-stimulated insulin secretion and content [19]. In our hands insulin release tended to be decreased upon ciRS-7 silencing, but not insulin content, partially confirming the observations of Xu et al. [19]. We observed a similar phenotype in MIN6B1 cells upon silencing ciRS-7 using a different siRNA ruling out the possibility of off-target effects mediated by the siRNA. Altogether, the functional impact we observed upon modulating ciRS-7 level is in line with a diabetes phenotype.

CircHIPK3 is one of the most abundant circRNAs present in pancreatic islets. This circRNA originates from exon 2 of *Hipk3*, a gene displaying diminished expression in the islets of Type 2 diabetic patients [34]. We found that linear *Hipk3* is decreased in both *ob/ob* and *db/db* mice, confirming a potential involvement in diabetes development. Shojima et al. observed that glucose-stimulated insulin secretion and content are reduced in *Hipk3*<sup>-/-</sup> mice and in isolated islets in which linear *Hipk3* is silenced [35]. Using our siRNA against linear *Hipk3*, we did not find a significant decrease in insulin secretion, but we confirmed a reduction in insulin content accompanied by a decrease in the insulin promoter activity. The phenotype of *Hipk3*<sup>-/-</sup> mice may at least in part be linked to the absence of circHIPK3. Indeed, the before mentioned publication does not provide any information about the region that has been deleted in *Hipk3*<sup>-/-</sup> mice. Therefore, these animals may lack exon 2 and hence circHIPK3. Moreover, as discussed below, even if this is not the case, the absence of linear *Hipk3* may indirectly result in a decrease in circHIPK3 levels. Besides its effect on insulin secretion, we found that silencing of linear *Hipk3* in MIN6B1 cells causes a rise in the apoptotic rate. These findings are consistent with the protective effect of HIPK3 against apoptosis observed in prostate cancer cells [50].

The expression of circHIPK3 is decreased in the islets of diabetic *db/db* mice, which display reduced insulin content, a diminished capacity to secrete insulin in response to glucose, and  $\beta$ -cell atrophy [20,51]. Silencing of circHIPK3 in  $\beta$ -cells resulted in a similar phenotype, suggesting that the drop in the level of this circular transcript may contribute to the events occurring during Type 2 Diabetes development.

Reduction of circHIPK3 levels using a siRNA induces apoptosis and decreases prolactin-stimulated  $\beta$ -cell proliferation. An analogous effect on proliferation was reported in several other human cell lines [15,43]. In contrast, silencing of circHIPK3 in bladder cancer cells increases migration and tumor invasion [38]. This effect was proposed to be exerted by sequestering miR-558, which is not expressed in  $\beta$ -cells. Thus, circHIPK3 may accomplish cell-specific tasks according to the presence or absence of particular interaction partners. In addition to the effects on  $\beta$ -cell survival, silencing of circHIPK3 led to defective glucose-induced insulin secretion. Moreover, modulation of circHIPK3 levels modified the insulin content by regulating the activity of the insulin promoter of MIN6B1 cells but not of rat islets. This may be explained by the fact that primary  $\beta$ -cells contain much higher insulin levels compared to cell lines and may be less affected by relatively small and acute decreases in insulin biosynthesis.

To elucidate the mode of action of circHIPK3, we investigated the transcriptional changes occurring upon silencing of this circular transcript. This resulted in the down-regulation of numerous genes involved in insulin secretion and PI3K-Akt signalling. AKT plays major roles in glucose-stimulated insulin secretion, apoptosis, and is a key player in the PI3K-pathway regulating  $\beta$ -cell proliferation [52]. Silencing of circHIPK3 also resulted in a decrease in *Mtpn* expression, an important component of the machinery controlling insulin secretion [26], and of *Slc2a2* encoding Glut2, an essential transporter for glucose uptake in  $\beta$ -cells [53]. Thus, the microarray data are in line with the observed phenotype and give some insight into the mode of action of circHIPK3.

The observed changes in gene expression can potentially be caused in *cis* or in *trans*. A computational analysis revealed that the genes downregulated upon circHIPK3 silencing are enriched for the targets of several miRNAs, including miR-124-3p, miR-29-3p, miR-338-3p, and miR-30, which have known functions in  $\beta$ -cells. In fact, miR-29 family members, as well as, miR-124-3p regulate insulin secretion [26,42]. In contrast, blockade of miR-338-3p promotes  $\beta$ -cell proliferation and survival under pro-apoptotic conditions [40,54], and miR-30 family members are involved in islet differentiation [44]. Interestingly, circHIPK3 was previously shown to directly bind to miR-124-3p, miR-29b-3p, and miR-338-3p [15], and other studies reported interactions of this circular transcript with miR-30 and miR-558 [38,43]. Hence, the functional effects of circHIPK3 silencing might at least in part be mediated by a consequent increase in the repressive activity of these miRNAs. In agreement with this hypothesis, we found that circHIPK3 modulates the expression of a luciferase reporter containing the 3'UTR of *MTPN*, which is controlled by miR-124-3p [26].

Silencing of linear and circular *Hipk3* transcripts have different impacts on gene expression pointing to a different mode of action despite sharing similar functional effects. However, in  $\beta$ -cells the expression of circular and linear *Hipk3* appears to be tightly interconnected. Using the same siRNA sequence used in this study, several groups working in different other cell types [15,43] did not report changes in linear *Hipk3* upon silencing of circHIPK3. Thus, the tight interconnection between circular and linear *Hipk3* expression may be a cell-type specific feature. Certain circRNAs share miRNA seed sites with the 3'UTR of their parent gene [16,55]. This enables them to control the level of their corresponding linear isoforms by sequestering the miRNAs and preventing their repressive activity. The sequence of circHIPK3 contains seed sites for numerous miRNAs present in the 3'UTR of *Hipk3* mRNA that may contribute to the coordination of the expression of the circular and linear transcripts. Another possible mechanism linking linear and circular *Hipk3* expression involves the regulation of the *Hipk3* promoter. Indeed, the product of the *Hipk3* gene is a kinase that phosphorylates different transcription factors including c-Jun. Since phosphorylated c-Jun activates the *Hipk3* promoter [50], this might elicit a feedforward cycle that sustains the expression of the gene. Thus, silencing of *Hipk3* may potentially lead to a reduction in the *Hipk3* promoter activity, and consequently, to a concurrent knockdown of circHIPK3.

## 5. CONCLUSION

We found that circRNAs are abundant in human islets and are conserved between species. CiRS-7 and circHIPK3 contribute to the regulation of essential  $\beta$ -cell activities and display altered expression in diabetes models, suggesting that they may be implicated in the development of this disease. A better understanding of the role of these newly discovered forms of RNA promises to shed new light on the

mechanisms causing  $\beta$ -cell failure under diabetic conditions and may lead to the discovery of new strategies to prevent or treat this very common metabolic disorder.

### ACKNOWLEDGEMENTS

This work was supported by grants of the Swiss National Science Foundation (310030-169480 (RR)), by the “Fondation Francophone pour la Recherche sur le Diabète” sponsored by the “Fédération Française des Diabétiques”, AstraZeneca, Eli Lilly, Merck Sharp & Dohme, Novo Nordisk and Sanofi (RR), and the National Health and Medical Research Council of Australia.

### APPENDIX A. SUPPLEMENTARY DATA

Supplementary data related to this article can be found at <https://doi.org/10.1016/j.molmet.2018.01.010>.

### AUTHOR CONTRIBUTION

LS generated and analyzed the research data, wrote the manuscript and approved its final version. JS, AR-T, CG, KL, MTV, JK and DRL contributed to the acquisition or the analysis of the data, reviewed the manuscript and approved its final version. RR conceived the experiments, analyzed the research data, wrote the manuscript and approved its final version.

### CONFLICT OF INTEREST

The authors declare no competing interest.

### REFERENCES

- Heit, J.J., Karnik, S.K., Kim, S.K., 2006. Intrinsic regulators of pancreatic beta-cell proliferation. *Annual Review of Cell and Developmental Biology* 22: 311–338.
- van Belle, T.L., Coppieters, K.T., von Herrath, M.G., 2011. Type 1 diabetes: etiology, immunology, and therapeutic strategies. *Physiological Reviews* 91: 79–118.
- Rahelic, D., 2016. 7th edition of *Idf diabetes Atlas—Call for immediate action*. *Lijecnicki Vjesnik* 138:57–58.
- Motterle, A., Gattesco, S., Caille, D., Meda, P., Regazzi, R., 2015. Involvement of long non-coding RNAs in beta cell failure at the onset of type 1 diabetes in NOD mice. *Diabetologia* 58:1827–1835.
- Guay, C., Jacovetti, C., Nesca, V., Motterle, A., Tugay, K., Regazzi, R., 2012. Emerging roles of non-coding RNAs in pancreatic beta-cell function and dysfunction. *Diabetes, Obesity and Metabolism* 14(Suppl. 3):12–21.
- Jeck, W.R., Sorrentino, J.A., Wang, K., Slevin, M.K., Burd, C.E., Liu, J., et al., 2013. Circular RNAs are abundant, conserved, and associated with ALU repeats. *RNA* 19:141–157.
- Salzman, J., Gawad, C., Wang, P.L., Lacayo, N., Brown, P.O., 2012. Circular RNAs are the predominant transcript isoform from hundreds of human genes in diverse cell types. *PLoS One* 7:e30733.
- Zhang, Y., Zhang, X.O., Chen, T., Xiang, J.F., Yin, Q.F., Xing, Y.H., et al., 2013. Circular intronic long noncoding RNAs. *Molecular Cell* 51:792–806.
- Pamudurti, N.R., Bartok, O., Jens, M., Ashwal-Fluss, R., Stottmeister, C., Ruhe, L., et al., 2017. Translation of CircRNAs. *Molecular Cell* 66, 9–21 e27.
- Li, Z., Huang, C., Bao, C., Chen, L., Lin, M., Wang, X., et al., 2015. Exon-intron circular RNAs regulate transcription in the nucleus. *Nature Structural & Molecular Biology* 22:256–264.
- Zlotorynski, E., 2015. Non-coding RNA: circular RNAs promote transcription. *Nature Reviews Molecular Cell Biology* 16:206.
- Du, W.W., Yang, W., Liu, E., Yang, Z., Dhaliwal, P., Yang, B.B., 2016. Foxo3 circular RNA retards cell cycle progression via forming ternary complexes with p21 and CDK2. *Nucleic Acids Research* 44:2846–2858.
- Lasda, E., Parker, R., 2014. Circular RNAs: diversity of form and function. *RNA* 20:1829–1842.
- Guo, J.U., Agarwal, V., Guo, H., Bartel, D.P., 2014. Expanded identification and characterization of mammalian circular RNAs. *Genome Biology* 15:409.
- Zheng, Q., Bao, C., Guo, W., Li, S., Chen, J., Chen, B., et al., 2016. Circular RNA profiling reveals an abundant circHIPK3 that regulates cell growth by sponging multiple miRNAs. *Nature Communications* 7:11215.
- Li, F., Zhang, L., Li, W., Deng, J., Zheng, J., An, M., et al., 2015. Circular RNA ITCH has inhibitory effect on ESCC by suppressing the Wnt/beta-catenin pathway. *Oncotarget* 6:6001–6013.
- Yang, W., Du, W.W., Li, X., Yee, A.J., Yang, B.B., 2016. Foxo3 activity promoted by non-coding effects of circular RNA and Foxo3 pseudogene in the inhibition of tumor growth and angiogenesis. *Oncogene* 35:3919–3931.
- Du, W.W., Yang, W., Liu, E., Yang, Z., Dhaliwal, P., Yang, B.B., 2016. Foxo3 circular RNA retards cell cycle progression via forming ternary complexes with p21 and CDK2. *Nucleic Acids Research* 44:2846–2858.
- Xu, H., Guo, S., Li, W., Yu, P., 2015. The circular RNA Cdr1as, via miR-7 and its targets, regulates insulin transcription and secretion in islet cells. *Scientific Reports* 5:12453.
- Chan, J.Y., Luzuriaga, J., Bensellam, M., Biden, T.J., Laybutt, D.R., 2013. Failure of the adaptive unfolded protein response in islets of obese mice is linked with abnormalities in beta-cell gene expression and progression to diabetes. *Diabetes* 62:1557–1568.
- Gotoh, M., Maki, T., Satomi, S., Porter, J., Bonner-Weir, S., O'Hara, C.J., et al., 1987. Reproducible high yield of rat islets by stationary in vitro digestion following pancreatic ductal or portal venous collagenase injection. *Transplantation* 43:725–730.
- Lilla, V., Webb, G., Rickenbach, K., Maturana, A., Steiner, D.F., Halban, P.A., et al., 2003. Differential gene expression in well-regulated and dysregulated pancreatic beta-cell (MIN6) sublines. *Endocrinology* 144:1368–1379.
- Motterle, A., Gattesco, S., Peyot, M.L., Esguerra, J.L.S., Gomez-Ruiz, A., Laybutt, D.R., et al., 2017. Identification of islet-enriched long non-coding RNAs contributing to beta-cell failure in type 2 diabetes. *Molecular Metabolism* 6:1407–1418.
- Veno, M.T., Hansen, T.B., Veno, S.T., Clausen, B.H., Grebing, M., Finsen, B., et al., 2015. Spatio-temporal regulation of circular RNA expression during porcine embryonic brain development. *Genome Biology* 16:245.
- Abderrahmani, A., Niederhauser, G., Favre, D., Abdelli, S., Ferdaoussi, M., Yang, J.Y., et al., 2007. Human high-density lipoprotein particles prevent activation of the JNK pathway induced by human oxidised low-density lipoprotein particles in pancreatic beta cells. *Diabetologia* 50:1304–1314.
- Sebastiani, G., Po, A., Miele, E., Ventriglia, G., Ceccarelli, E., Bugliani, M., et al., 2015. MicroRNA-124a is hyperexpressed in type 2 diabetic human pancreatic islets and negatively regulates insulin secretion. *Acta Diabetologica* 52:523–530.
- Agarwal, V., Bell, G.W., Nam, J.W., Bartel, D.P., 2015. Predicting effective microRNA target sites in mammalian mRNAs. *Elife* 4.
- Abuelo, A., Hernandez, J., Alves-Nores, V., Benedito, J.L., Castillo, C., 2016. Association of serum concentration of different trace elements with biomarkers of systemic oxidant status in dairy cattle. *Biological Trace Element Research* 174:319–324.
- Memczak, S., Jens, M., Elefsinioti, A., Torti, F., Krueger, J., Rybak, A., et al., 2013. Circular RNAs are a large class of animal RNAs with regulatory potency. *Nature* 495:333–338.
- Wang, Y., Liu, J., Liu, C., Naji, A., Stoffers, D.A., 2013. MicroRNA-7 regulates the mTOR pathway and proliferation in adult pancreatic beta-cells. *Diabetes* 62:887–895.

- [31] Latreille, M., Hausser, J., Stutzer, I., Zhang, Q., Hastoy, B., Gargani, S., et al., 2014. MicroRNA-7a regulates pancreatic beta cell function. *Journal of Clinical Investigation* 124:2722–2735.
- [32] Xu, H., Guo, S., Li, W., Yu, P., 2015. The circular RNA Cdr1as, via miR-7 and its targets, regulates insulin transcription and secretion in islet cells. *Scientific Reports* 5:12453.
- [33] Suzuki, H., Tsukahara, T., 2014. A view of pre-mRNA splicing from RNase R resistant RNAs. *International Journal of Molecular Sciences* 15:9331–9342.
- [34] Locke, J.M., da Silva Xavier, G., Dawe, H.R., Rutter, G.A., Harries, L.W., 2014. Increased expression of miR-187 in human islets from individuals with type 2 diabetes is associated with reduced glucose-stimulated insulin secretion. *Diabetologia* 57:122–128.
- [35] Shojima, N., Hara, K., Fujita, H., Horikoshi, M., Takahashi, N., Takamoto, I., et al., 2012. Depletion of homeodomain-interacting protein kinase 3 impairs insulin secretion and glucose tolerance in mice. *Diabetologia* 55:3318–3330.
- [36] Ng, S.F., Lin, R.C., Maloney, C.A., Youngson, N.A., Owens, J.A., Morris, M.J., 2014. Paternal high-fat diet consumption induces common changes in the transcriptomes of retroperitoneal adipose and pancreatic islet tissues in female rat offspring. *The FASEB Journal* 28:1830–1841.
- [37] Perry, J.R., McCarthy, M.I., Hattersley, A.T., Zeggini, E., Wellcome Trust Case Control, C., Weedon, M.N., et al., 2009. Interrogating type 2 diabetes genome-wide association data using a biological pathway-based approach. *Diabetes* 58:1463–1467.
- [38] Li, Y., Zheng, F., Xiao, X., Xie, F., Tao, D., Huang, C., et al., 2017. CircHIPK3 sponges miR-558 to suppress heparanase expression in bladder cancer cells. *EMBO Reports*.
- [39] Sebastiani, G., Po, A., Miele, E., Ventriglia, G., Ceccarelli, E., Bugliani, M., et al., 2015. MicroRNA-124a is hyperexpressed in type 2 diabetic human pancreatic islets and negatively regulates insulin secretion. *Acta Diabetologica* 52:523–530.
- [40] Jacovetti, C., Jimenez, V., Ayuso, E., Laybutt, R., Peyot, M.L., Prentki, M., et al., 2015. Contribution of intronic miR-338-3p and its hosting gene AATK to compensatory beta-cell mass expansion. *Molecular Endocrinology* 29:693–702.
- [41] Pullen, T.J., da Silva Xavier, G., Kelsey, G., Rutter, G.A., 2011. miR-29a and miR-29b contribute to pancreatic beta-cell-specific silencing of monocarboxylate transporter 1 (Mct1). *Molecular and Cellular Biology* 31:3182–3194.
- [42] Roggli, E., Gattesco, S., Caille, D., Briet, C., Boitard, C., Meda, P., et al., 2012. Changes in microRNA expression contribute to pancreatic beta-cell dysfunction in prediabetic NOD mice. *Diabetes* 61:1742–1751.
- [43] Shan, K., Liu, C., Liu, B.H., Chen, X., Dong, R., Liu, X., et al., 2017. Circular non-coding RNA HIPK3 mediates retinal vascular dysfunction in diabetes mellitus. *Circulation* 136:1629–1642.
- [44] Ozcan, S., 2014. Minireview: microRNA function in pancreatic beta cells. *Molecular Endocrinology* 28:1922–1933.
- [45] Tan, J.Y., Marques, A.C., 2016. miRNA-mediated crosstalk between transcripts: the missing “linc”? *BioEssays* 38:295–301.
- [46] Dong, W.W., Li, H.M., Qing, X.R., Huang, D.H., Li, H.G., 2016. Identification and characterization of human testis derived circular RNAs and their existence in seminal plasma. *Scientific Reports* 6:39080.
- [47] Wang, P.L., Bao, Y., Yee, M.C., Barrett, S.P., Hogan, G.J., Olsen, M.N., et al., 2014. Circular RNA is expressed across the eukaryotic tree of life. *PLoS One* 9: e90859.
- [48] Hansen, T.B., Jensen, T.I., Clausen, B.H., Bramsen, J.B., Finsen, B., Damgaard, C.K., et al., 2013. Natural RNA circles function as efficient microRNA sponges. *Nature* 495:384–388.
- [49] Piwecka, M., Glazar, P., Hernandez-Miranda, L.R., Memczak, S., Wolf, S.A., Rybak-Wolf, A., et al., 2017. Loss of a mammalian circular RNA locus causes miRNA deregulation and affects brain function. *Science* 357 eaam8526.
- [50] Curtin, J.F., Cotter, T.G., 2004. JNK regulates HIPK3 expression and promotes resistance to Fas-mediated apoptosis in DU 145 prostate carcinoma cells. *The Journal of Biological Chemistry* 279:17090–17100.
- [51] Kjørholt, C., Akerfeldt, M.C., Biden, T.J., Laybutt, D.R., 2005. Chronic hyperglycemia, independent of plasma lipid levels, is sufficient for the loss of beta-cell differentiation and secretory function in the db/db mouse model of diabetes. *Diabetes* 54:2755–2763.
- [52] Elghazi, L., Balcazar, N., Bernal-Mizrachi, E., 2006. Emerging role of protein kinase B/Akt signaling in pancreatic beta-cell mass and function. *The International Journal of Biochemistry & Cell Biology* 38:157–163.
- [53] Guillam, M.T., Hummler, E., Schaerer, E., Yeh, J.I., Birnbaum, M.J., Beermann, F., et al., 1997. Early diabetes and abnormal postnatal pancreatic islet development in mice lacking Glut-2. *Nature Genetics* 17:327–330.
- [54] Jacovetti, C., Abderrahmani, A., Parnaud, G., Jonas, J.C., Peyot, M.L., Cornu, M., et al., 2012. MicroRNAs contribute to compensatory beta cell expansion during pregnancy and obesity. *Journal of Clinical Investigation* 122: 3541–3551.
- [55] Yang, W., Du, W.W., Li, X., Yee, A.J., Yang, B.B., 2015. Foxo3 activity promoted by non-coding effects of circular RNA and Foxo3 pseudogene in the inhibition of tumor growth and angiogenesis. *Oncogene* 55:3919–3931.